 doi:10.20944/preprints202205.0118.v1

Article

Synthesis of magnetic bioactive composites thought bio-inspired surface modification

Alexander Volov[1], Lubov Shkodenko[2], Elena I. Koshel[2] and Andrey S. Drozdov[3]*

[1] Department of Chemistry, Moscow State University, Moscow, Russia volovalexander@gmail.com
[2] SCAMT Institute, ITMO University, Saint Petersburg, Russia
[3] Laboratory of Nanobiotechnologies, Moscow Institute of Physics and Technology, Dolgoprudny, Moscow Region, Russia
* Correspondence: drozdov.science@gmail.com

Abstract: Organically-coated nanomaterials are intensively studied and find numerous applications in a wide range of areas ranging from optics to biomedicine. One of the recent trends in material science is the application of bio-mimetic polydopamine coatings that can be produced on a variety of substrates in a cost-efficient way under mild conditions. Such coatings not only modify the biocompatibility of the material but also add functional amino groups to the surface that can be further modified by classic conjugation techniques. Here we show an alternative strategy of substrates modification using not dopamine but dopamine conjugates. Compared to the classic scheme the proposed strategy allows for separation of the "organic" and "colloidal" stages and simplifies identification and purification steps. Modification with pre-modified dopamine allowed to achieve high active components loading up to 10.5% wt. A series of organo-inorganic hybrids were synthesized and their bioactivity was analyzed.

Keywords: magnetite; dopamine; surface modification; hybrid materials, antibacterial agents.

1. Introduction

It can be concluded without any hesitation that the most important points for material development are related to the creation of materials with the desired bulk properties and the appropriate surface properties. Both these issues determine the potency and effectiveness of the potential systems and should be carefully optimized for material to achieve its desired functions. The balance between these two depends on the proposed application scenarios but when it comes to bioactive materials the importance of surface properties is becoming dominant due to the complexity and versatility of the interactions on the biointerface[1–4]. A large number of methods of both physical and chemical nature were developed for surface modification for specialized applications[5–9]. The current trend in surface modification strategies is aimed at simplification and universalization of the approaches and softening reaction conditions. In 2007 Lee *et al.* described a universal coating strategy inspired by the attachment of mussels to various surfaces[10]. Proteomic analysis has discovered that the attachment of mussels is mediated through adhesive foot protein, Mefp-5 (Mytilus edulis foot protein-5) rich in 3,4-dihydroxy-L-phenylalanine (DOPA) and lysine, bearing catechol- and amino-groups correspondingly, which are strongly interacting with each other and surface functional groups through hydrogen bonds, electrostatic and hydrophobic interactions ensuring strong attachment to almost all type of surfaces, both organic and inorganic, including super-hydrophobic ones. This discovery led to the development of so-called polydopamine (PDA) coatings which are readily formed in mild conditions through oxidative cyclization and polymerization of dopamine by soluted oxygen[11–15]. Due to relative cheapness, biocompatibility and synthetic availability bio-inspired coatings have found their applications in various fields of science, such as cell patterning, theranostics,

 doi:10.20944/preprints202205.0118.v1

tissue engineering, photocatalysis, and Li-ion batteries[15–17]. Another important feature is that such self-forming coatings that bear amino groups can be further modified by typical chemical approaches to functionalize the surface with desired agents[18–20]. As an alternative to post-synthetic modification of the surface substrates can be modified by pre-functionalized coatings. This strategy allows separating the process of synthesis into three stages: synthesis of substrates, such as nanoparticles by the means of colloid chemistry; synthesis of functional monomers by conventional organic synthesis and application of the coating on the substrate's surface. This approach potentially not only simplifies the characterization and purification but also allows for improving the ratio between used-for-the-synthesis and immobilized functional agents as well as conjugating agents compared to typical synthesis-coating-modification strategy as the latter method typically requires large excesses of reagents for successful functionalization. Several articles described were devoted to the modification of nanoparticles with dopamine derivatives but still, this approach gained much fever attention compared to classic strategy[21–23]. Here we attempted to highlight the potency of using pre-modified dopamine for the creation of functional nanocomposites. Since PDA coatings may be formed on almost any type of surface we chose magnetite nanoparticles as a substrate due to their unique magnetic properties and excellent biocompatibility. We synthesized several dopamine conjugates and compared the effectiveness of modification whit these agents on three types of magnetite nanoparticles. The dependencies of the modification results on the synthetic conditions and bioactivity of the synthesized composites on model systems are presented.

2. Results

2.1. Magnetic nanoparticles

Initial affords were aimed at finding an optimal nanoparticle to be used for further modifications. Among the great variety of the known magnetic nanosystems, we decided to consider three types of magnetite nanoparticles in order to define the best and most convenient one. The first system was magnetite hydrosol (Ferria) which was described earlier in our works[24,25]. This system was a hydrocolloid of octahedron-shaped magnetite nanoparticles with a mean diameter of 10 nm dispersed in deionized water with excellent colloidal stability at a neutral pH level without any added surface modifying agents or peptization agents in its composition. Due to the non-stochiometric ratio of Fe(II) and Fe(III) ions during its synthesis the surface of nanoparticles is enriched with Fe(II)-OH groups that shift the isoelectric point the material from typical for magnetite pH 6.8 [26] to pH 8.2 resulting in the highly positive zeta potential of the system valued +32 mV at neutral pH level[25,27].

Preprints (www.preprints.org) | NOT PEER-REVIEWED | Posted: 9 May 2022 doi:10.20944/preprints202205.0118.v1

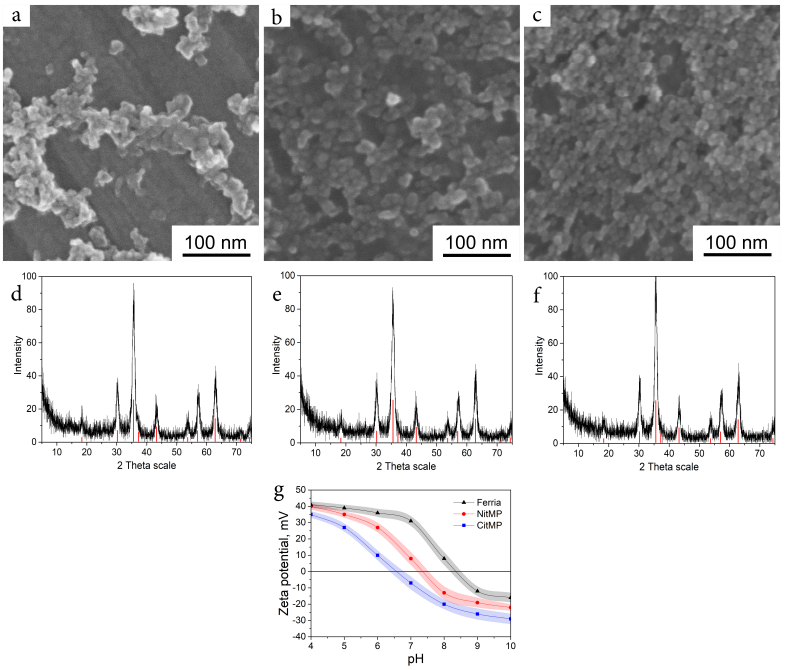

Figure 1. Magnetite nanoparticles in this study. SEM image and XRD pattern of Ferria (A,D), NitMP (B,E), and NitMP (C,F). G: Zeta potential at various pH levels for all synthesized hydrocolloids.

Two more magnetite hydrosols were used to evaluate the effect of surface chemistry on the effectiveness of biomimetic surface modification. The second tested system was well-known and widely applied citrate-capped magnetite nanoparticles hydrosol (CitMP). This type of magnetite hydrocolloid is based on the ability of citric anion to coordinate on the surface of magnetite nanoparticles by two carboxylic and one hydroxyl group resulting in highly charged and stable hydrosols[28–31]. The third system was another typical and well-described magnetic colloid that consisted of magnetite hydrosol which was stabilized by nitric acid (NitMP). Nitric acid is a well-known peptization agent widely applied in sol-gel chemistry to charge surfaces of nanoparticles by increasing H^+ concentration near their surface[32,33]. All named systems have been synthesized by co-precipitation procedures thus all had near-spherical shapes as was seen from SEM images (Figure 1A-C). All three materials had almost identical XRD patterns (Figure 1D-F) that demonstrated the main peak at 35.58° attributed to the crystalline plane with Miller indices of (311) as well as other distinctive peaks at 18.36° (111), 30.10° (220), 43.25° (400), 53.66° (422), 57.20° (511), 62.82° (440), 71.28° (620), and 74.33° (533) typical for magnetite crystalline phase (RRUFF No.R061111). The crystallite sizes were calculated by the Scherrer equation and were valued between 10 and 11 nm proving the propinquity of the synthesized nanoparticles parameters. The main difference between the named systems was the approach to their stabilization that resulted in differences in their surface chemistry and hydrodynamic parameters (Table 1). The most striking difference between used systems can be seen in their isoelectric points valued at 6.3 to 7.3 and 8.2 for CitMP, NitMP, and Ferria respectively (Table 1 and Figure 1E). This difference originated from the nature of their surface charge: while for NitMP and Ferria the charge originated from Fe-OH hydroxyl groups on the surface, for CitMP it is also affected by carboxylic groups of citrate residues on the surface of nanoparticles that shifts isoelectric point to lower pH. The comparative characteristics of the used systems can be seen in Table 1

 doi:10.20944/preprints202205.0118.v1

Table 1. Magnetite hydrosols used in this study.

Name	pH of the colloid	Surface groups	Crystallite diameter, nm	Hydrodynamic radius, nm	Isoelectric point, pH	ζ potential at
CitMP	4.6	-COOH	10.47	40	6.3	-7
NitMP	2.3	Fe-OH_2^+	10.74	38	7.3	+8
Ferria	6.8	Fe(II)-OH_2^+	10.31	33	8.2	+31

2.2. Biomimetic coating of the nanoparticles

The surface of the synthesized NPs was modified via biomimetic polymerization of dopamine derivatives. In the initial experiments, the applicability of dopamine derivatives for this process was evaluated. For this purpose firstly we compared the effectiveness of nanoparticle modification by dopamine and dopamine conjugate with glycine (GlyDop) at various pH levels. The coating efficiency for both catechols showed nonlinear dependence on pH level with a local maximum near pH 8, which correlates with previously published data[34,35]. The effectiveness of coating with unmodified dopamine for used nanoparticle substrates was nearly identical at acidic pH levels and showed a minor difference in the basic pH region resulting in up to 42.8%, 37.94% and 36.1% GlyDop absorption for Ferria, NitMP and CitMP respectively (Fig. 2A). For GlyDop coating more pronounced dependence on the NPs surface charge and chemistry was observed (Fig. 2B) with much higher efficiency for Ferria NPs reaching 53.6% at pH 8.0, while for NitMP and CitMP these values were 43.9% and 34.1% respectively.

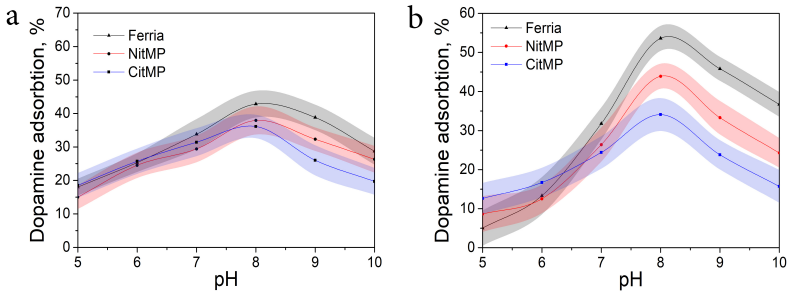

Figure 2. Adsorption of dopamine (A) and GlyDop (B) on nanoparticles as a function of pH level.

This was additionally proved by TGA measurements of the resulted composites, which demonstrated the mass fraction of polydopamine coating in Ferria@GlyDop, NitMP@GlyDop, and CitMP@GlyDop at the level of 32% 28% and 21% wt. respectively (Fig. 3A-C) corresponding to 10.5% 9.3% and 7% wt. of glycine correspondingly.

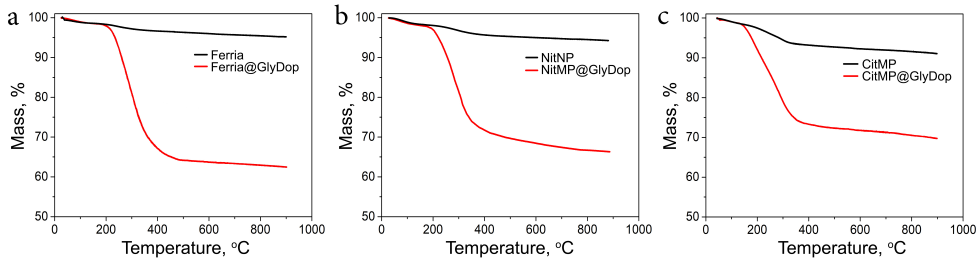

Figure 3. TGA curves of Ferria (A), NitMP (B) and CitMP (C) and the corresponding composites with GlyDop.

2.3. Bioactivity of the dopamine-coated NPs

Biomimetic modification of nanoparticles offers a quick and convenient strategy for surface engineering and may be used to alternate the bioactivity of nanoparticle

Preprints (www.preprints.org) | NOT PEER-REVIEWED | Posted: 9 May 2022 doi:10.20944/preprints202205.0118.v1

systems. To evaluate this possibility two systems were prepared and their bioactivity was tested on bacteria models. In the first model, MNPs were modified with the conjugate of dopamine and arabinose (AraDop), and the bioavailability of the material was evaluated on *E. coli* Nova Blue pBad strain which was genetically designed to produce Green Fluorescent Protein (GFP) when arabinose is added to the nutrient media. The concentration of GFP was measured as a fluorescence intensity at 532 nm, thus allowing for evaluating the bioactivity of the systems. The results are presented in Figure 4. All the tested systems caused the appearance of a fluorescent signal which showed a direct dependence on arabinose species concentrations. The conjugated form of arabinose caused approximately two and four times lower biological response for AraDop and AraDop@Ferria compared to free Ara on all the tested concentrations in the range from 0.01 to 1 mg/mL.

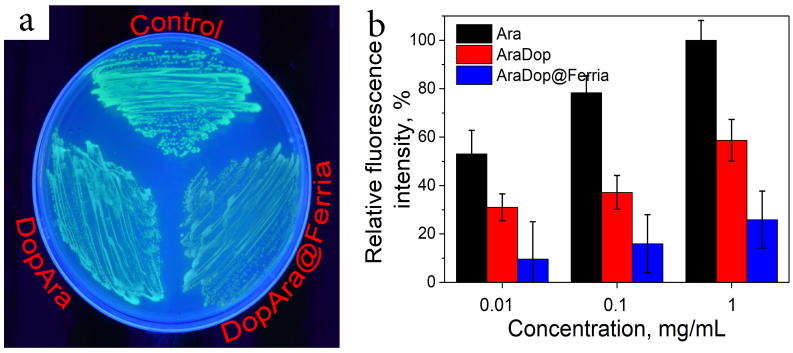

Figure 4. Bioactivity of AraDop@Ferria. A: Visual appearance of fluorescent *E.coli* Nova Blue pBad; (*E.coli* Nova Blue pBad; B: Fluorescent signal in response to various arabinose species.

As the second model system, we have selected Ferria NPs modified with ampicillin-dopamine conjugate AmpDop@Ferria and evaluated its antibacterial activity on ampicillin sensitive *E. coli* ATCC 25922 (Figure 5). Based on the results of the experiment, we can conclude that the antibacterial activity of conjugated ampicillin decreased compared to its free form. In the experiment with the conjugate, the minimum inhibitory concentrations (MIC) were found at 5 and 10 μg/mL for AmpDop and AmpDop@Ferria correspondingly, while for free ampicillin MIC was found at the level of 2 μg/mL, while control experiments showed absence of any antibacterial activity for dopamine or Ferria.

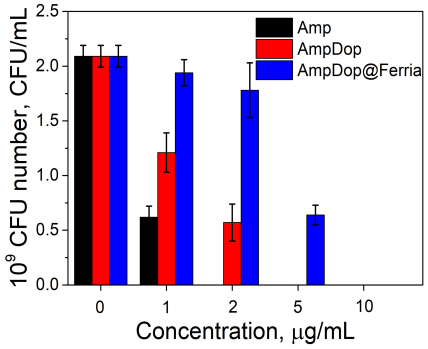

Figure 5. Antibiotic activity of AmpDop@Ferria.

3. Discussion

Here we showed the potency of the biomimetic strategy of nanoparticles surface modification by dopamine derivatives *in-situ* polymerization under mild conditions for the production of bioactive nanocomposites. This strategy relies on oxidative cyclization of dopamine under mild conditions resulting in its polymerization as it is shown in Figure 6. The exact mechanism behind the process remains unknown, but its main

Preprints (www.preprints.org) | NOT PEER-REVIEWED | Posted: 9 May 2022 doi:10.20944/preprints202205.0118.v1

features are broadly discussed in the literature[12,36,37]. In the first step, dopamine is oxidized by dissolved oxygen forming a quinone intermediate. The formed quinone can undergo intramolecular cyclization leading to 5,6-dihydroxyindole (DHI), the second important molecule. It is thought that these two compounds and initial dopamine can interact in various ways, including covalent inter-molecular bonding leading to melanin- and eumelanin-like structures and non-covalent self-assembly through hydrophobic interactions, hydrogen bonds, and π-π stacking[12,13]. The overall PDA layer formation process consists of two processes: dopamine polymerization and its adsorption to the surface.

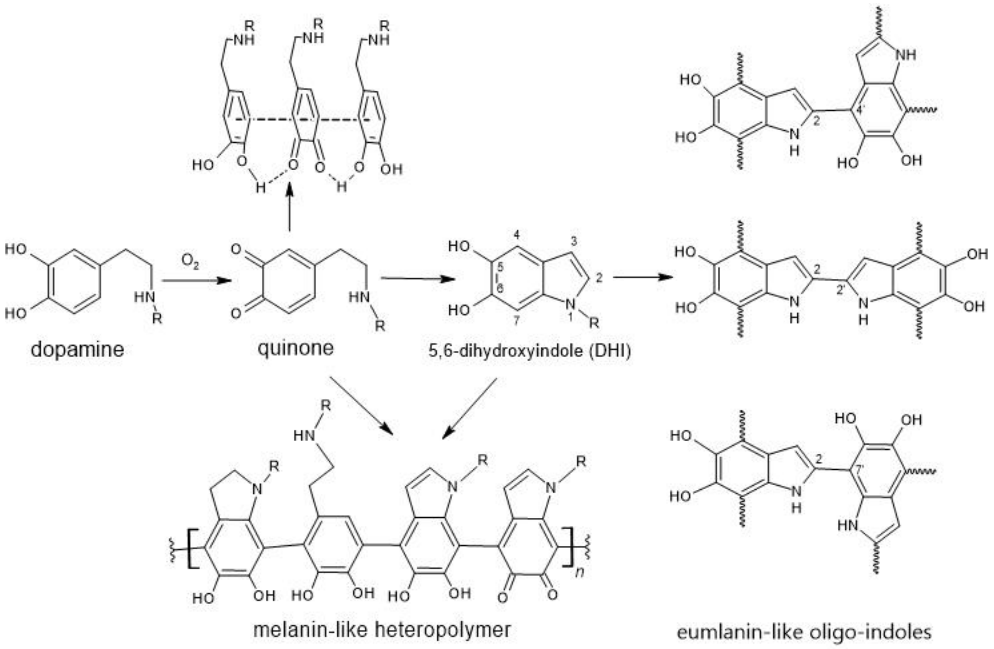

Figure 6. Schematic representation of dopamine polymerization

It is known that bidentate catechols such as dopamine and its derivatives effectively bind to iron oxide primary through dissociated catechol groups converting under-coordinated Fe-O surface sites back to an octahedral bulk-like lattice structure. The effectiveness of this process is dependent on the surface chemistry. Generally, the thickness of the formed surface correlates with the hydrophobicity of the surface and its charge in the reaction conditions[13]. It is known that a higher negative charge of the surface inhibits the rate of adsorption of the dissociated catechol groups leading to lower rates of nucleation and deposition of organic polymer. This fact had founded its reflected in our study. We used three types of iron oxide with equal hydrodynamic radius but different surface properties, namely magnetite nanoparticles coated with citric acid (CitMP), nitric acid (NitMP), and iron hydroxide (Ferria). Comparative PDA layer deposition under the same conditions showed lower effectiveness in the row Ferria>NItMP>CitMP following the decline in the substrate isoelectric point and higher negative charge of the surface. As was shown in the literature and mentioned earlier, the rate of PDA deposition is dependent on several aspects: catechol adsorption, quinone and 5,6 dihydroindole formation rate, formation of melanin- and eumelanin-like polymer and its nucleation. All of these processes are occurring through protonation and deprotonation the pH level plays an important role in the process of PDA layer formation. It is known that the monomer formation rate is accelerating at a higher pH level. At the same time, it was found that high pH levels lower the effectiveness of PDA deposition due to dissociation of phenolic hydroxyls at their pK_a point near pH 9.0-9.5. Since catechols surface adsorption is the primary step in the mechanism of polydopamine layer formation, dissociation of catechols at higher pH becomes a dominant effect that

 doi:10.20944/preprints202205.0118.v1

favors dissolution rather than adsorption[38]. This phenomenon was also observed in our case when the effectiveness of the modification of all the tested systems was maximal at pH 8.0, while higher pH levels lowered the level of NPs modification. It was demonstrated that biomimetic modification of NPs surface via dopamine derivatives can be used for the synthesis of bioactive composite materials in a fast and convenient way. Separation of the whole process into two distinct stages done by the means of organic and colloidal chemistry gives better control over each of them and potentially allows to combine of more complex systems by using several dopamine derivatives simultaneously during the polymerization stage. In addition, this approach can lead to higher loading capacities of the NPs with bioactive molecules which reached in the case of GlyDop up to 10.5% due to volume deposition of bioactive molecules, while the effectiveness of typical post-deposition surface modification strategies is typically limited by 1-3% due to fact that conjugation is done only on an NPs surface while the modification or packing densities may be as low as 0.01-0.5 molecules per square nanometer[39–41]. The bioactivity of the magnetic nanoparticles can be modulated by the attachment of dopamine conjugates. In this study, we demonstrated that Ferria can be made either biocidal or biofriendly by modification with AmpDop or AraDop conjugate correspondingly. Conjugation of ampicillin and arabinose to dopamine led to an approximately two-fold decrease in their activity, and organo-inorganic composites showed even lower activity which was five and four folds lower than free molecules at maximal tested concentrations, while at low concentrations their activities were even lower. The decrease of biological activity and such concentration-dependent behavior can be associated with lower bioavailability of molecules bound to nanoparticles' surfaces due to low internalization rates of the modified nanoparticles[42,43]. Slow degradation rates of the organic coatings within bacteria also could play a role in lowering the bioactivity of the composites, but nevertheless, these preliminary results proved the conception and will be further investigated in the future.

4. Conclusions

Here we demonstrated the concept of nanoparticle surface modification based on pre-synthesized dopamine conjugates. Magnetic nanoparticles were modified with dopamine conjugates under mild conditions leading to organo-inorganic composites with a high rate of the organic component. Application of dopamine conjugates allowed to achieve high active molecules loading up to 10.5% wt. The synthesized systems demonstrated bioactivity inherent to the used dopamine conjugates. The contingency of the modification process and bioactivity of the synthesized materials proved the potency of the proposed strategy, which will be further evaluated in the upcoming works.

5. Materials and Methods

Chemicals: All reagents and solvents were obtained or distilled according to standard procedures. The reagents used for experiments were purchased from Sigma-Aldrich Co. and used as received unless otherwise noted. N,N-dimethylformamide (DMF), acetonitrile, 1,4-dioxane, and tetrahydrofuran (THF) were distilled from phosphorus pentoxide under argon, and solvents were stored under argon.

Bacterial Strains: E. coli strain ATCC 25922 and *E. coli* XL1 Blue carrying plasmid pBADcycle3-mutant strains were grown at 37 °C in lysogeny broth (LB) medium supplemented with 12.5 μg/mL of tetracycline (PanReac AppliChem, Barcelona, Spain).

*Magnetite hydrosol (**Ferria**):* Stable magnetite hydrosol was prepared by the procedure described earlier.[24,44] Briefly, 2.5 g $FeCl_2$*$4H_2O$ and 5 g $FeCl_3$*$6H_2O$ were dissolved in 100 mL of deionized water. Then, 11 mL of 30% NH_4OH was added under constant stirring (500 rpm) at room temperature. The formed magnetite precipitate was magnetically separated and washed with deionized water until neutral pH. The washed black precipitate was mixed with 100 mL of deionized water and subjected to

Preprints (www.preprints.org) | NOT PEER-REVIEWED | Posted: 9 May 2022 doi:10.20944/preprints202205.0118.v1

ultrasonic treatment (37 kHz, 110 W) under constant stirring (300 rpm). The resulting mass concentration of the magnetite hydrosol was 2%.

*Nitric acid stabilized magnetite (**NitMP**):* Nanoparticles were synthesized according to the procedure from ref. [45]. Briefly, 5.9 g of $FeCl_3$*$6H_2O$ and 2.15 g of $FeCl_2$*$4H_2O$ were dissolved in 100 mL of degassed deionized water. 12.5 mL of 30% NH_4OH was quickly added. The solution was heated to 85 °C and stirred for 1 h. Then the formed magnetic particles were magnetically separated and washed sequentially with 2 M HNO_3 and thrice with deionized water. The resulting suspension was diluted with deionized water to the final mass concentration of 2% wt.

*Citric acid stabilized magnetite (**CitMP**):* Nanoparticles were synthesized as described in ref. [46]. Briefly, $FeCl_2$*$4H_2O$ (2.5 g) and $FeCl_3$*$6H_2O$ (4.0 g) were dissolved in 180 mL of distilled water under nitrogen gas. 50 mL of sodium hydroxide was dropwise added to the reaction mixture and kept for 10 min at 65 °C under continuous vigorous stirring. Then, 150 mL of 5% citric acid solution was added to the reaction mixture, which was then stirred for 10 min (65 °C). CitMP was collected with a permanent magnet and thoroughly rinsed four times with distilled water. The resulting suspension was diluted with deionized water to the final mass concentration of 2% wt.

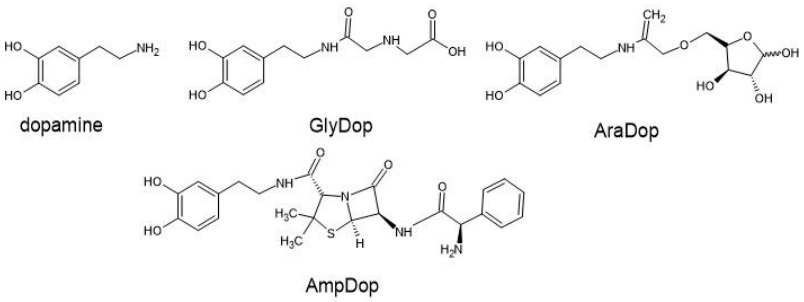

Figure 7. Structures of dopamine and dopamine derivatives in this study

N-Chloroacetyl-3,4-dihydroxyphenethylamine: To an aqueous solution of dopamine hydrochloride (1.89 g, 10 mmol) was added, under nitrogen, 25 mL of 2.0 N sodium hydroxide and then an ethereal solution of chloroacetic anhydride (1.71 g, 15.2 mmol). Vigorous stirring was continued for 0.5 hr. More sodium hydroxide (10 mL, 2 equiv) and 1.71 g of chloroacetic anhydride were added under stirring. The reaction mixture was kept stirring for 1 hr more. The reaction mixture was neutralized to pH 6 by the addition of hydrochloric acid and extracted with ethyl acetate four times. The combined extracts left an oily residue, 2.4 g, which was chromatographed on a column of 45 g of silica gel. The column was eluted with chloroform containing 4% methanol, and fractions of 7 ml were collected. Fractions 30-50 contained pure N-chloroacetyl-3,4-dihydroxyphenethylamine which was recrystallized from chloroform to yield colorless crystalline granules (1.52 g, 67% yield), mp 108-109 °C. HRMS for $C_10H_12ClNO_3$ [M+H]+ Calc.: 231.0476, found: 231.0462

*(2-((3,4-dihydroxyphenethyl)amino)-2-oxoethyl)glycine (**GlyDop**):* To a solution of N-Chloroacetyl-3,4-dihydroxyphenethylamine (1 g, 4.4 mmol) in 1,4-dioxane (20 mL) was added, under nitrogen, 25 mL of 2.0 N sodium hydroxide and then p-tosylglycine (1 g, 4.4 mmol). Vigorous stirring was continued for 3 hr. The reaction mixture was neutralized to pH 1 by the addition of hydrochloric acid and extracted with ethyl acetate four times. The organic extracts were combined and dried over MgSO4, filtered and evaporated in vacuo. The crude residue was purified by column chromatography (silica, $CHCl_3$-MeOH (5:1)) to give the target product (820 mg, 70% yield). 1H NMR (600 MHz, MeOD) σ 7.87-7.84 (2H, m, ArH), 7.51-7.46 (1H, m, ArH), 3.50 (2H, t, J=7.3 Hz, CH2N), 3.46 (2H, s, CH2), 3.22 (2H, s, CH2), 2.74 (2H, t, J=7.3 Hz, CH2Ar); 13C NMR (150 MHz, MeOD) σ 173.1, 170.7, 145.6, 144.5, 131.5, 122.8, 116.4, 52.9, 50.7, 40.3, 39.4 HRMS for $C_12H_16N_2O_5$ [M+H]+ Calc.: 269.1093, found: 269.1087

 doi:10.20944/preprints202205.0118.v1

*Conjugate of dopamine with arabinose (**AraDop**):* A suspension of D-arabinose (0.5 g, 3.33 mmol) and potassium carbonate (0.69 g, 5 mmol) in anhydrous acetonitrile (15 ml) was stirred at room temperature under N2 atmosphere for 15 min. Then N-Chloroacetyl-3,4-dihydroxyphenethylamine (0.76 g, 3.33 mmol) was added, and stirring was prolonged for 12 h. The reaction was monitored by TLC using petroleum hexane/ethyl acetate 1:2 (v/v) as the eluent. The solvent was removed under reduced pressure and the residue purified by flash silica gel column chromatography using hexane/ethyl acetate 1:2 (v/v) as the eluent to yield conjugate (540 mg, 87% yield). Mp 112-114 °C; 1H NMR (600 MHz, MeOD) σ 7.85-7.82 (2H, m, ArH), 7.50-7.46 (1H, m, ArH), 5.85-5.83 (1H, m, H-1'), 4.59-4.56 (1H, m, H-4'), 4.50-4.48 (1H, m, H-3'), 4.42-4.40 (1H, m, 3'-OH), 4.32-4.29 (1H, m, 2'-OH), 3.91-3.88 (1H, m, H-2'), 3.59-3.56 (1H, m, 5'-CH2), 3.55 (2H, s, CH2), 3.47 (2H, t, J=7.3 Hz, CH2N), 3.36-3.34 (1H, m, 5'-CH2), 2.75 (2H, t, J=7.3 Hz, CH2Ar); 13C NMR (150 MHz, MeOD) σ 168.6, 145.3, 144.7, 131.5, 122.8, 116.4, 115.9, 102.7, 84.0, 76.7, 76.5, 72.0, 68.8, 40.6, 39.4 HRMS for $C_15H_21NO_8$ [M+H]+ Calc.: 344.1301, found: 344.1324

*Conjugate of dopamine with ampicillin (**AmpDop**):* A solution of ampicillin (0.5 g, 1.43 mmol) and CDI (0.42 g, 2.58 mmol) in anhydrous DMF (15 mL) was stirred at room temperature under N2 atmosphere for 15 min. Then dopamine (0.27 g, 1.43 mmol) was added, and stirring was prolonged for 12 h. The reaction was monitored by TLC using petroleum ether/ethyl acetate 2:8 (v/v) as the eluent. The solvent was removed under reduced pressure and the residue was purified by flash silica gel column chromatography using petroleum ether/ethyl acetate 2:8 (v/v) as the eluent to yield conjugate (600 mg, 87% yield). Mp 99-102 °C; 1H NMR (600 MHz, MeOD) σ 8.72 (2H, s, NH2), 7.85-7.82 (2H, m, ArH), 7.50-7.46 (1H, m, ArH), 7.39-7.36 (2H, m, ArH), 7.34-7.32 (1H, m, ArH), 7.30-7.27 (2H, m, ArH), 5.22-5.19 (1H, m, CH), 4.87-4.84 (1H, m, CH), 4.82-4.78 (1H, m, CH), 3.47 (2H, t, J=7.3 Hz, CH2N), 2.75 (2H, t, J=7.3 Hz, CH2Ar), 1.58 (3H, s, CH3), 1.53 (3H, s, CH3); 13C NMR (150 MHz, MeOD) σ 174.5, 171.0, 169.2, 145.6, 144.5, 133.6, 131.5, 129.6, 129.2, 127.6, 122.8, 116.4, 115.9, 87.0, 71.8, 65.0, 60.7, 57.2, 40.6, 39.4, 29.4, 29.2 HRMS for $C_24H_28N_4O_5S$ [M+H]+ Calc.: 485.1814, found: 485.1822

PDA layer formation on MNPs: For PDA layer formation experiments 100 μL of magnetite NPs was mixed with 100 μL of 2% dopamine derivative solution in methanol and 200 μL of PBS or acetate buffer with the desired pH was added. The system was incubated for 24 hours, magnetically separated, and washed six times with 100 μL of a buffer. The collected liquid fraction was analyzed with UV spectroscopy.

Antibiotic activity testing: The strain of E. coli ATCC 25922, which is sensitive to ampicillin, was used for the experiment. 5 μL of bacteria suspension was added to test tubes with 1 mL LB of nutrient medium and cultured for 24 hours. After that, the tested substance was added and the culture was grown for another 24 hours in 1 mL of LB culture medium for 24 hours at 37 °C in a shaker incubator at 250 rpm and optical density was measured.

Bacteria biofluorescence experiments: 5 μL of bacteria suspension was added to test tubes with 1 mL LB of nutrient medium and cultured for 24 hours. After that, the tested substance was added and the culture was grown for another 24 hours in 1 mL of LB culture medium for 24 hours at 37 °C in a shaker incubator at 250 rpm and fluorescence was measured.

Author Contributions: "Conceptualization, A.D.; formal analysis, E.K. and A.D.; experiments, A.V., L.S., E.K., and A.D.; writing A.D.

Funding: This research was funded by the Russian Science Foundation, grant number 20-73-00001

Conflicts of Interest: The authors declare no conflict of interest

References

1. Zhu, N.; Ji, H.; Yu, P.; Niu, J.; Farooq, M.; Akram, M.W.; Udego, I.; Li, H.; Niu, X. Surface modification of magnetic iron oxide nanoparticles. *Nanomaterials* **2018**, *8*, 810.

2. Neděla, O.; Slepička, P.; Švorčík, V. Surface modification of polymer substrates for biomedical applications. *Materials* **2017**, *10*, 1115.
3. Barui, A.K.; Oh, J.Y.; Jana, B.; Kim, C.; Ryu, J.H. Cancer-targeted nanomedicine: Overcoming the barrier of the protein corona. *Advanced therapeutics* **2020**, *3*, 1900124.
4. Drozdov, A.S.; Nikitin, P.I.; Rozenberg, J.M. Systematic Review of Cancer Targeting by Nanoparticles Revealed a Global Association between Accumulation in Tumors and Spleen. *International Journal of Molecular Sciences* **2021**, *22*, 13011.
5. Kango, S.; Kalia, S.; Celli, A.; Njuguna, J.; Habibi, Y.; Kumar, R. Surface modification of inorganic nanoparticles for development of organic–inorganic nanocomposites—A review. *Progress in Polymer Science* **2013**, *38*, 1232–1261.
6. Kaseem, M.; Fatimah, S.; Nashrah, N.; Ko, Y.G. Recent progress in surface modification of metals coated by plasma electrolytic oxidation: Principle, structure, and performance. *Progress in Materials Science* **2021**, *117*, 100735.
7. Lam, M.; Migonney, V.; Falentin-Daudre, C. Review of silicone surface modification techniques and coatings for antibacterial/antimicrobial applications to improve breast implant surfaces. *Acta Biomaterialia* **2021**, *121*, 68–88.
8. Zhang, J.; Mou, L.; Jiang, X. Surface chemistry of gold nanoparticles for health-related applications. *Chemical Science* **2020**, *11*, 923–936.
9. Nemani, S.K.; Annavarapu, R.K.; Mohammadian, B.; Raiyan, A.; Heil, J.; Haque, M.A.; Abdelaal, A.; Sojoudi, H. Surface modification of polymers: methods and applications. *Advanced Materials Interfaces* **2018**, *5*, 1801247.
10. Lee, H.; Dellatore, S.M.; Miller, W.M.; Messersmith, P.B. Mussel-inspired surface chemistry for multifunctional coatings. *science* **2007**, *318*, 426–430.
11. Qiu, W.Z.; Yang, H.C.; Xu, Z.K. Dopamine-assisted co-deposition: an emerging and promising strategy for surface modification. *Advances in Colloid and Interface Science* **2018**, *256*, 111–125.
12. Ryu, J.H.; Messersmith, P.B.; Lee, H. Polydopamine surface chemistry: a decade of discovery. *ACS applied materials & interfaces* **2018**, *10*, 7523–7540.
13. Klosterman, L.; Riley, J.K.; Bettinger, C.J. Control of heterogeneous nucleation and growth kinetics of dopamine-melanin by altering substrate chemistry. *Langmuir* **2015**, *31*, 3451–3458.
14. Lee, H.A.; Park, E.; Lee, H. Polydopamine and its derivative surface chemistry in material science: a focused review for studies at KAIST. *Advanced Materials* **2020**, *32*, 1907505.
15. Liebscher, J.; Mrowczynski, R.; Scheidt, H.A.; Filip, C.; Hadade, N.D.; Turcu, R.; Bende, A.; Beck, S. Structure of polydopamine: a never-ending story? *Langmuir* **2013**, *29*, 10539–10548.
16. Ball, V. Polydopamine nanomaterials: recent advances in synthesis methods and applications. *Frontiers in bioengineering and biotechnology* **2018**, *6*, 109.
17. Palladino, P.; Bettazzi, F.; Scarano, S. Polydopamine: surface coating, molecular imprinting, and electrochemistry—successful applications and future perspectives in (bio) analysis. *Analytical and bioanalytical chemistry* **2019**, *411*, 4327–4338.
18. Ding, Y.; Floren, M.; Tan, W. Mussel-inspired polydopamine for bio-surface functionalization. *Biosurface and biotribology* **2016**, *2*, 121–136.
19. Ye, Q.; Zhou, F.; Liu, W. Bioinspired catecholic chemistry for surface modification. *Chemical Society Reviews* **2011**, *40*, 4244–4258.
20. Liu, C.Y.; Huang, C.J. Functionalization of polydopamine via the aza-michael reaction for antimicrobial interfaces. *Langmuir* **2016**, *32*, 5019–5028.
21. Barclay, T.G.; Hegab, H.M.; Clarke, S.R.; Ginic-Markovic, M. Versatile surface modification using polydopamine and related polycatecholamines: Chemistry, structure, and applications. *Advanced Materials Interfaces* **2017**, *4*, 1601192.
22. Lee, H.A.; Ma, Y.; Zhou, F.; Hong, S.; Lee, H. Material-independent surface chemistry beyond polydopamine coating. *Accounts of chemical research* **2019**, *52*, 704–713.
23. Mazur, M.; Barras, A.; Kuncser, V.; Galatanu, A.; Zaitzev, V.; Turcheniuk, K.V.; Woisel, P.; Lyskawa, J.; Laure, W.; Siriwardena, A.; others. Iron oxide magnetic nanoparticles with versatile surface functions based on dopamine anchors. *Nanoscale* **2013**, *5*, 2692–2702.
24. Shapovalova, O.E.; Drozdov, A.S.; Bryushkova, E.A.; Morozov, M.I.; Vinogradov, V.V. Room-temperature fabrication of magnetite-boehmite sol-gel composites for heavy metal ions removal. *Arabian Journal of Chemistry* **2020**, *13*, 1933–1944.
25. Drozdov, A.S.; Ivanovski, V.; Avnir, D.; Vinogradov, V.V. A universal magnetic ferrofluid: Nanomagnetite stable hydrosol with no added dispersants and at neutral pH. *Journal of colloid and interface science* **2016**, *468*, 307–312.

26. Kosmulski, M. The pH dependent surface charging and points of zero charge. VII. Update. *Advances in Colloid and Interface Science* **2018**, *251*, 115–138.
27. Anastasova, E.I.; Ivanovski, V.; Fakhardo, A.F.; Lepeshkin, A.I.; Omar, S.; Drozdov, A.S.; Vinogradov, V.V. A pure magnetite hydrogel: synthesis, properties and possible applications. *Soft matter* **2017**, *13*, 8651–8660.
28. Qureashi, A.; Pandith, A.H.; Bashir, A.; Manzoor, T.; Malik, L.A.; Sheikh, F.A. Citrate coated magnetite: A complete magneto dielectric, electrochemical and DFT study for detection and removal of heavy metal ions. *Surfaces and Interfaces* **2021**, *23*, 101004.
29. Liu, J.; Sun, Z.; Deng, Y.; Zou, Y.; Li, C.; Guo, X.; Xiong, L.; Gao, Y.; Li, F.; Zhao, D. Highly water-dispersible biocompatible magnetite particles with low cytotoxicity stabilized by citrate groups. *Angewandte Chemie International Edition* **2009**, *48*, 5875–5879.
30. Andreeva, Y.I.; Drozdov, A.S.; Fakhardo, A.F.; Cheplagin, N.A.; Shtil, A.A.; Vinogradov, V.V. The controllable destabilization route for synthesis of low cytotoxic magnetic nanospheres with photonic response. *Scientific reports* **2017**, *7*, 1–9.
31. RuizMoreno, R.; Martinez, A.; Castro-Rodriguez, R.; Bartolo, P. Synthesis and characterization of citrate coated magnetite nanoparticles. *Journal of superconductivity and novel magnetism* **2013**, *26*, 709–712.
32. Mérida, F.; Chiu-Lam, A.; Bohórquez, A.C.; Maldonado-Camargo, L.; Pérez, M.E.; Pericchi, L.; Torres-Lugo, M.; Rinaldi, C. Optimization of synthesis and peptization steps to obtain iron oxide nanoparticles with high energy dissipation rates. *Journal of magnetism and magnetic materials* **2015**, *394*, 361–371.
33. Mandel, K.; Szczerba, W.; Thünemann, A.F.; Riesemeier, H.; Girod, M.; Sextl, G. Nitric acid-stabilized superparamagnetic iron oxide nanoparticles studied with X-rays. *Journal of nanoparticle research* **2012**, *14*, 1–9.
34. Salomaki, M.; Marttila, L.; Kivela, H.; Ouvinen, T.; Lukkari, J. Effects of pH and oxidants on the first steps of polydopamine formation: a thermodynamic approach. *The Journal of Physical Chemistry B* **2018**, *122*, 6314–6327.
35. Alfieri, M.L.; Panzella, L.; Oscurato, S.L.; Salvatore, M.; Avolio, R.; Errico, M.E.; Maddalena, P.; Napolitano, A.; d'Ischia, M. The chemistry of polydopamine film formation: the amine-quinone interplay. *Biomimetics* **2018**, *3*, 26.
36. Ding, Y.; Weng, L.T.; Yang, M.; Yang, Z.; Lu, X.; Huang, N.; Leng, Y. Insights into the aggregation/deposition and structure of a polydopamine film. *Langmuir* **2014**, *30*, 12258–12269.
37. Yang, J.; Stuart, M.A.C.; Kamperman, M. Jack of all trades: versatile catechol crosslinking mechanisms. *Chemical Society Reviews* **2014**, *43*, 8271–8298.
38. Bernsmann, F.; Ersen, O.; Voegel, J.C.; Jan, E.; Kotov, N.A.; Ball, V. Melanin-containing films: growth from dopamine solutions versus layer-by-layer deposition. *ChemPhysChem* **2010**, *11*, 3299–3305.
39. Tan, J.; Cho, T.J.; Tsai, D.H.; Liu, J.; Pettibone, J.M.; You, R.; Hackley, V.A.; Zachariah, M.R. Surface modification of cisplatin-complexed gold nanoparticles and its influence on colloidal stability, drug loading, and drug release. *Langmuir* **2018**, *34*, 154–163.
40. Cinier, M.; Petit, M.; Williams, M.N.; Fabre, R.M.; Pecorari, F.; Talham, D.R.; Bujoli, B.; Tellier, C. Bisphosphonate adaptors for specific protein binding on zirconium phosphonate-based microarrays. *Bioconjugate chemistry* **2009**, *20*, 2270–2277.
41. Queffelec, C.; Petit, M.; Janvier, P.; Knight, D.A.; Bujoli, B. Surface modification using phosphonic acids and esters. *Chemical reviews* **2012**, *112*, 3777–3807.
42. Kumar, A.; Pandey, A.K.; Singh, S.S.; Shanker, R.; Dhawan, A. Cellular uptake and mutagenic potential of metal oxide nanoparticles in bacterial cells. *Chemosphere* **2011**, *83*, 1124–1132.
43. Jayawardena, H.S.N.; Jayawardana, K.W.; Chen, X.; Yan, M. Maltoheptaose promotes nanoparticle internalization by Escherichia coli. *Chemical Communications* **2013**, *49*, 3034–3036.
44. Kolchanov, D.S.; Slabov, V.; Keller, K.; Sergeeva, E.; Zhukov, M.V.; Drozdov, A.S.; Vinogradov, A.V. Sol–gel magnetite inks for inkjet printing. *Journal of Materials Chemistry C* **2019**, *7*, 6426–6432.
45. Nikitin, M.P.; Shipunova, V.O.; Deyev, S.M.; Nikitin, P.I. Biocomputing based on particle disassembly. *Nature nanotechnology* **2014**, *9*, 716–722.
46. Dheyab, M.A.; Aziz, A.A.; Jameel, M.S.; Noqta, O.A.; Khaniabadi, P.M.; Mehrdel, B. Simple rapid stabilization method through citric acid modification for magnetite nanoparticles. *Scientific reports* **2020**, *10*, 1–8.

 doi:10.20944/preprints202205.0118.v1

 doi:10.20944/preprints202205.0118.v1